

# Machine learning for recovery factor estimation of an oil reservoir: a tool for de-risking at a hydrocarbon asset evaluation

Ivan Makhotin<sup>a</sup>, Denis Orlov<sup>a</sup>, Dmitry Koroteev<sup>a</sup>, Evgeny Burnaev<sup>a</sup>, Aram Karapetyan<sup>b</sup>, Dmitry Antonenko<sup>b</sup>

<sup>a</sup>*Skolkovo Institute of Science and Technology, Moscow, Russia*

<sup>b</sup>*JSC Zarubezhneft, Moscow, Russia*

---

## Abstract

Well known oil recovery factor estimation techniques such as analogy, volumetric calculations, material balance, decline curve analysis, hydrodynamic simulations have certain limitations. Those techniques are time-consuming, require specific data and expert knowledge. Besides, though uncertainty estimation is highly desirable for this problem, the methods above do not include this by default. In this work, we present a data-driven technique for oil recovery factor of hydrocarbon reservoirs using parameters and various representative statistics. We apply advanced machine learning methods using extensive historical worldwide oilfields datasets (more than 2000 oil reservoirs). The data-driven model might be used as a general tool for rapid and completely objective estimation of the oil recovery factor. In addition, it includes the ability to work with partial input data and to estimate the prediction interval of the oil recovery factor. We perform the evaluation in terms of accuracy and prediction intervals coverage for several tree-based machine learning techniques in application to the following two cases: (1) using parameters only related to geometry, geology, transport, storage and fluid properties, (2) using an extended set of parameters including development and production data. For both cases model proved itself to be robust and reliable. We conclude that the proposed data-driven approach overcomes several limitations of the traditional methods and is suitable for rapid, reliable and objective estimation of oil recovery factor for hydrocarbon reservoir.

**Keywords:** Oil recovery factor, machine learning, regression, uncertainty estimation, conformal predictors, clustering, oilfield, oil reservoir

---

*Email addresses:* [Ivan.Makhotin@skoltech.ru](mailto:Ivan.Makhotin@skoltech.ru) (Ivan Makhotin), [D.Orlov@skoltech.ru](mailto:D.Orlov@skoltech.ru) (Denis Orlov), [D.Koroteev@skoltech.ru](mailto:D.Koroteev@skoltech.ru) (Dmitry Koroteev), [E.Burnaev@skoltech.ru](mailto:E.Burnaev@skoltech.ru) (Evgeny Burnaev), [AKarapetyan@nestro.ru](mailto:AKarapetyan@nestro.ru) (Aram Karapetyan), [DAntonenko@nestro.ru](mailto:DAntonenko@nestro.ru) (Dmitry Antonenko)

## 1. Introduction

When bidding for a license area for hydrocarbon exploration, operating companies need to evaluate an expected margin as accurate as possible. A significant portion of overall investment into an oilfield is spending to get as much a-priori information about a reservoir as possible. Estimation of expected oil recovery is essential for the asset evaluation and further field development planning. Oil recovery factor is critically affected by characteristics of the reservoir (geological structure, internal architecture, properties of reservoir rock and fluids) and the specifics of the oilfield development scheme [1]. There are several methods to estimate oil recovery factor with data collected from seismic surveying or acquisition of a previous surveying data, well logs, petrophysical studies and collection of production profiles.

Nowadays, most of the sedimentary basins that contain oil have been already explored, and discoveries tend to be small. It becomes relevant to choose the most cost-effective one among many possible options with varying completeness of data. That is why it is essential to estimate recoverable reserves of discoveries from available data rapidly and with uncertainty. There are methods which allow performing an estimate in early life of oilfield when there are no sufficient amount of production data and detailed hydrodynamic model. Such a field is sometimes referred to as greenfield. These methods are volumetric and analogy [2]. The analogy method requires representative oilfields database and highly depends on reservoir characteristics similarity. The main idea of the volumetric method is to estimate original oil in place with geological model that geometrically describes the volume of hydrocarbons in the reservoir. Along with this, oil recovery factor evaluation performing by estimating primary and secondary recovery. The primary recovery factor is often estimated mainly from predominant drive mechanism identification. The secondary recovery factor is estimated as the product of displacement efficiency and sweep efficiency. These terms are influenced by fluid flow properties, reservoir heterogeneity that may be measured with petrophysical studies and well logs. Both methods require a specific set of data, relatively time-consuming and do not provide uncertainty by default.

There are cases when it might be necessary to assess mature oilfield (sometimes referred to as brownfield). High amount of production data or relatively detailed hydrodynamic model allows obtaining an accurate and reliable reserves estimation using decline curve analysis, material balance or numerical hydrodynamic simulations [2]. Decline curve analysis refers to estimating reserves based on analysis of production characteristics only such as oil rate and oil-cut. Material balance and numerical hydrodynamic simulations are good in terms of capturing the major physical mechanisms of hydrocarbon filtration through a reservoir rock. However, these methods are relatively time-consuming, require significant efforts and detailed reservoir description to build an accurate model and even greater efforts to conduct uncertainty quantification.

Nowadays, different machine learning techniques are increasingly being applied in the oil and gas industry [3]. The data-driven approach allows retrieving

non-trivial dependencies and building powerful predictive models from historical data.

Several studies are demonstrating empirical relationships between known parameters at exploration phase and oil recovery factor. Guthrie et al. [4] obtained linear dependency of recovery factor for water drive reservoirs on its properties. Arps et al. [5] using the same data obtained non-linear relationships for water drive and solution gas drive reservoirs.

Recently, there were several attempts to apply machine learning to recovery factor estimation. Sharma et al. [6] were used Tertiary Oil Recovery Information System (TORIS) for oil reservoirs and the Gas Information System (GASIS) for gas reservoirs to fit multivariate linear regression. The authors demonstrate high accuracy of the linear model. However, less than 2% of TORIS oil reservoirs were used for training and testing. Mahmoud et al. [7] show the successful application of the artificial neural networks (ANNs) using descriptions of 130 water drive sandstone reservoirs. Han and Bian [8] demonstrate the application of a model based on support vector machine in combination with the particle swarm optimization (PSO-SVM) technique for oil recovery factor prediction using description of 34 low-permeable reservoirs. Aliyuda and Howell [9] demonstrate successful application of Support Vector Machine using 93 reservoirs descriptions from the Norwegian Continental Shelf as a dataset.

Machine learning contains a huge set of algorithms and allows to build predictive models taking into account the specifics of the problem. The objective of this study is to construct and evaluate a rapid, robust data-driven model (surrogate model, [10]) for oil recovery factor estimation with predictive uncertainty. Assessment often needed to be performed based on available data. Additional measurements and lab studies require additional time and resources. Accordingly, we are focus on methods that are capable of working with partial input data. Relatively rich available sources of data characterizing more than 2000 oil reservoirs from all over the world allow constructing representative training sample to attain strong generalization ability. We consider the application of machine learning algorithms based on trees ensembles which are well suited to problem specificity. Due to the varying level of completeness for reservoirs description, we provide separate analysis for greenfields and brownfields. Having a lack of oil production information in greenfield case, the data-driven uncertainty quantification model could help reservoir experts to assess the potential of the hydrocarbon reservoirs more objectively and reliably. For brownfield case, the data-driven model could help experts to optimize development plan as well as to validate results of the complex 4D hydrodynamic model.

## 2. Datasets

We consider two datasets. Both contain multi-feature oil reservoirs descriptions. The description includes time-independent measurements and parameters related to reservoir geometry, geology and petrophysical studies. It also contains a set of parameters which were measured at some moment during the production phases. Both datasets include estimated recovery factors, which

were estimated according to the development plans and measurements assuming secondary recovery methods. Overall, databases provide information about 2500 oil reservoirs all over the world.

### 2.1. TORIS dataset

Tertiary Oil Recovery Information System (TORIS) is a data repository which was originally developed by the National Petroleum Council (NPC) for its 1984 assessment of the USA enhanced oil recovery potential [6]. Dataset contains description of 1381 oil reservoirs from the USA. Number of parameters is 56. Among them 12 categorical and 44 numerical. Data contains incomplete records, 22% values are missing. Geographical layout is shown in Figure 1.

**TORIS dataset oil reservoirs location**

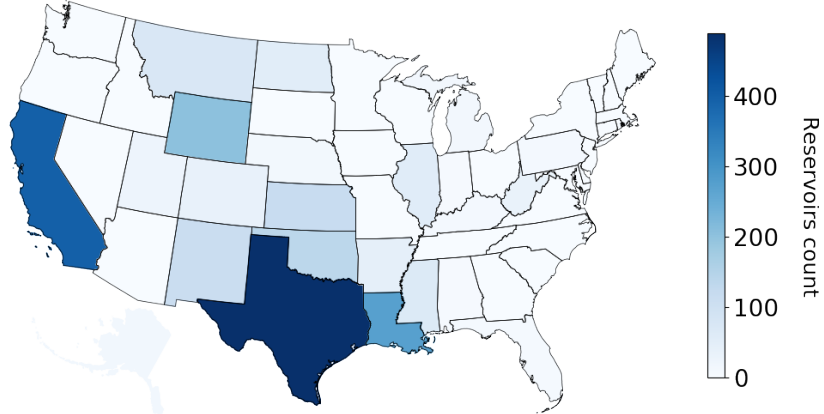


Figure 1: Oil reservoirs location from TORIS database

Only 831 of 1381 reservoirs contain oil recovery factor and can be used for training and evaluation. We group all parameters in the following way:

- Geometry — Field Acres, Proven Acres, Net Pay, Gross Pay, True Vertical Depth, Reservoir Acres, Reservoir Dip
- Geology — Lithology, Geologic Age, Fractured-Fault, Shale break of laminations, Major Gas Cap, Deposition System, Diagenetic Overprint, Structural Compartmentalization, Predominant Element of Reservoir Heterogeneity, Trap Type
- Transport, Storage and Fluid properties — Porosity, Permeability, Oil viscosity, Formation salinity, Clay content, Formation temperature, API Gravity
- Saturations, Ratios and Pressures — Initial & Current oil saturations, Initial & Current water saturations, Initial & Current gas saturations, Initial & Current oil formation volume factor, Initial & Current formation pressure, Initial & Current producing GOR

- Development and Production — Well Spacing, Production/Injection wells count, Swept Zone oil saturation (Residual to water), Injection water salinity, Dykstra-Parsons Coefficient, Current injection rate, Original oil in place, Production rate, Cumulative oil production, First stage oil recovery factor, Second stage oil recovery factor
- Location — State, Formation Name

## 2.2. Proprietary dataset

Another dataset has been provided by Russian oil company. It contains information about 1119 oil reservoirs throughout the world. This dataset provides more comprehensive descriptions in comparison to TORIS. Number of parameters is 199. Among them 74 categorical and 125 numerical. Data contains incomplete records, 38.5% values are missing. Geographical layout is shown in 2.

Proprietary dataset oil reservoirs location

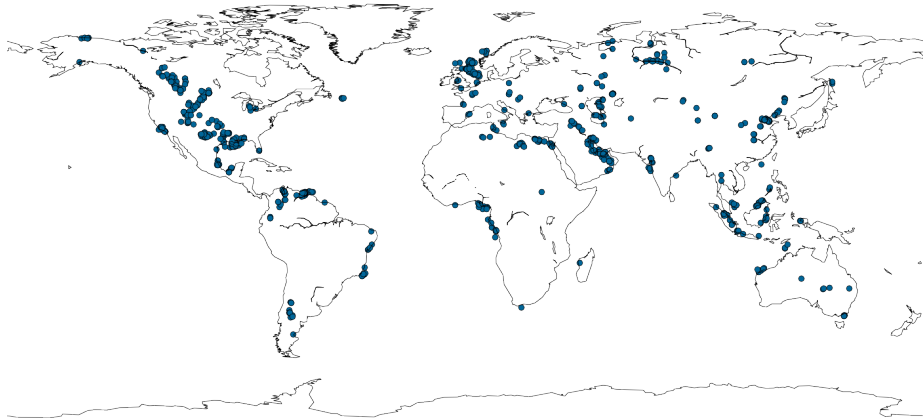


Figure 2: Oil reservoirs location from proprietary database

Only 737 of 1119 reservoirs contain secondary oil recovery factor and can be used for training and evaluation. We group all parameters in the following way:

- Geometry — Seal thickness, Elevation, Water depth, True Vertical Depth, Structural dip, Closure area, Closure height, Area (original productive), Fluid contact (original OWC/GOC/GWC), Hydrocarbon column height (original oil/gas/total), Thickness (gross pay, avg/min/max), Thickness (net pay, avg/min/max)
- Geology — Tectonic regime, Source rock depositional environment, Kerogen type, Seal rock (unit/period/epoch/age/depositional system/depositional

environment lithology/classification), Structural setting, Trapping mechanism (main/secondary/tertiary), Structural compartment count, Reservoir (period/epoch/age), Depositional system (main/secondary), Depositional environment (main/secondary/tertiary), Stratigraphic compartment count, Fracture origin (main/secondary), Lithology (main/secondary), Grain size for clastics (main/secondary), Depositional texture for carbonates (main/secondary), Depositional component for clastics/carbonates (main/secondary), Basin type, Diagenetic reservoir, Fracture reservoir type, Source rock (unit/period/epoch/age/lithology).

- Transport, Storage and Fluid properties — API gravity, Viscosity, Viscosity temperature, Gas specific gravity, Sulphur (%), Wax (%), Carbon dioxide (%), Hydrogen sulphide (%), Nitrogen (%), Gas-oil ratio, FVF, Temperature, Temperature depth, Water salinity, Porosity type (main/secondary/tertiary), Porosity (matrix/fracture, avg/min/max), Permeability (air, avg/min/max), Permeability (production-derived, avg/min/max)
- Saturations, Ratios and Pressures — Pressure (original), Pressure depth, Pressure (current), Pressure year (current), Pressure gradient (original), Pressure (saturation), Net-gross ratio (avg), Water saturation measurement source, Water saturation (avg/min/max, %)
- Development and Production — Reserves (original/recoverable in-place oil/gas/condensate), Production year (cumulative), Production (cumulative oil/gas/condensate), Production year (start), Production year (plateau), Production rate (plateau oil/gas/condensate), Production year (current), Well count (current, producing/injection), Water-cut (current, %), Production rate (current, oil/gas/condensate), Single well rate (max, oil/gas), Drive mechanism (main/secondary), Hydrocarbon type (main/secondary/tertiary), Improved recovery method (main/secondary/tertiary), Recovery factor (oil, primary/secondary/tertiary, %), Well spacing (oil/gas, average), Discovery year, Reservoir status (current), Well count (total, production/injection), Seismic anomaly, Unconventional reservoir type
- Location — Field name, Operator company, Reservoir unit, Basin name, Latitude, Longitude, Onshore or offshore, Country, State, Region

### 3. Background

#### 3.1. Problem statement

The general problem statement of this study is to infer the statistical relationship between secondary recovery factor of an oil reservoir and its observed parameters. In more formal way, let  $X = \{x_i\}_{i=1}^n \in \mathbf{X}^n \subset \mathbb{R}^{n \times d}$  denotes numerical description of the oil reservoirs, where  $n$  is the number of reservoirs and  $d$  is the number of observed variables. Let  $Y = \{y_i\}_{i=1}^n \in \mathbf{Y}^n \subset \mathbb{R}^n$  denotes column of response variables. In our case  $Y$  becomes the column of secondary oil recovery factors for the corresponding reservoirs. Having available

data  $z_1 = (x_1, y_1), \dots, z_n = (x_n, y_n)$ , confidence level  $\alpha$  and new oil reservoir description  $x$  our purpose is to construct prediction interval  $\Gamma^\alpha(z_1, \dots, z_n, x)$  which satisfy the following proprieties:

**Validity**

Prediction set  $\Gamma^\alpha(z_1, \dots, z_n, x)$  is valid if it contains true  $y$  with probability not less than  $\alpha$ .

**Efficiency**

Prediction set  $\Gamma^\alpha(z_1, \dots, z_n, x)$  is efficient if the prediction interval is usually relatively small and therefore informative.

Since we have noisy data and significant portion of values are missing it is quite natural to consider machine learning algorithms based on decision trees such as Random Forests and Gradient Boosting over decision trees. These models proved itself to be robust to noise, able to handle missing values and sufficiently accurate for engineering applications. In this study we provide evaluation of two tree-based algorithms: Quantile Regression Forests and Gradient boosting over decision trees with Inductive Conformal Predictors.

### 3.2. Models based on decision trees

In this section we briefly describe ensemble regression meta-algorithms, which use decision tree as base estimator. The equation (1) represents ensemble meta-algorithm as weighted sum of base estimators  $b_k$ .

$$\hat{f}(x) = \sum_{k=1}^T \omega_k b_k(x). \quad (1)$$

Decision tree is a supervised learning method. It derives decision rules recursively from data. Decision tree building algorithm works top-down. At every node it chooses the best variable and threshold that splits current training subset in the best way according to selected homogeneity measure of the target variable within the subsets. The process is recursively repeated until some limit on the number of items in the node is not achieved. The terminal nodes are called leaves. After the tree is built, it can determine to which leaf the new item belongs using logical rules. Prediction for it will be weighted mean of the training subset targets of this leaf.

#### 3.2.1. Quantile Regression Forests

Random Forests were initially introduced by Breiman [11]. It is a powerful tool for high-dimensional regression and classification problems. Random forests is the modification of bagging [12]. In bagging approach every base estimator uses as training set random subset of samples and in some modifications random subset of features. All weights  $\omega_k$  are equal to  $\frac{1}{T}$  and  $b_k$  are trained independently (Eq. 1). The difference of Random Forest from bagging is that splitting value is selected from random subset at every node. Robustness of the Random Forests to outliers and noisy variables is associated with this randomness. Classical Random Forests regression tries to give a point estimate  $\hat{\mu}(x)$  of the response variable  $y$ , given  $x$ . However, it is shown that random Random

Forests provides information about the full conditional distribution of the response variable [13]. Authors show that Random Forests allows to approximate full conditional distribution  $\hat{F}(y|x)$ . Hence, we are able to estimate quantiles of the conditional distribution as  $\hat{Q}_q(x) = \inf\{y : \hat{F}(y|x) \geq q\}$ . Therefore, prediction interval could be computed as  $\Gamma^\alpha(z_1, \dots, z_n, x) = [\hat{Q}_{\frac{1-\alpha}{2}}(x), \hat{Q}_{\alpha+\frac{1-\alpha}{2}}(x)]$ . The algorithm is shown to be consistent. It was shown that under several assumptions error of the approximation to the conditional distribution converges uniformly in probability to zero for  $n \rightarrow \infty$  [13].

### 3.2.2. Inductive Conformal Predictors over Gradient Boosting

Unlike Random Forests, Gradient Boosting base estimators are trained sequentially. Each new one compensates for the residuals of the previous ones by learning the gradient of the loss function [14]. After the new base estimator has trained the appropriate weight  $\omega_k$  is selected with a simple one-dimensional optimization of the loss function. Since base estimators are dependent there are no any similar way to estimate conditional distribution of the response variable.

Conformal predictors is the meta-algorithm which can be built on top of almost any supervised machine learning algorithm [15]. It allows constructing prediction set for corresponding confidence level using any regression or classification method as underlying algorithm. Conformal predictors is defined using the concept of nonconformity measure. A nonconformity measure is a measurable function  $B : Z^* \times Z \rightarrow \mathbb{R}$ , such that  $B(\zeta, z)$  does not depend on the ordering of  $\zeta$ . Intuition:  $B(\zeta, z)$  (the nonconformity score) shows how different  $z$  from the examples in  $\zeta$ . Possible choice:

$$B(\zeta, (x, y)) = \Delta(y, \hat{f}(x)),$$

where  $f : \mathbf{X} \rightarrow \mathbf{Y}'$  — prediction rule founded from  $\zeta$  as the training set and  $\Delta : \mathbf{Y} \times \mathbf{Y}' \rightarrow \mathbb{R}$  — is a measure of similarity between the target and the prediction. In this study we used Inductive Conformal Predictors which is computationally efficient modification of the initial algorithm.

An inductive conformal predictor requires the following steps:

1. Split the training set into the proper training set  $z_1, \dots, z_m$  and calibration set  $z_{m+1}, \dots, z_l$ .

2. Find the prediction set for  $x$  at confidence level  $\alpha \in (0, 1)$ . For each  $y \in \mathbf{Y}$ :

- Compute the nonconformity scores (the raw prediction step)

$$\beta_i = B((z_1, \dots, z_m), z_i), i \in \{m+1, \dots, l\}$$

$$\beta^y = B((z_1, \dots, z_m), (x, y))$$

- Compute the p-value (the calibration step)

$$p(y) = \frac{|\{i = m+1, \dots, l : \beta_i \geq \beta^y\}| + 1}{l - m + 1}$$

Output the prediction set:

$$\Gamma^\alpha(z_1, \dots, z_n, x) = \{y : p(y) > 1 - \alpha\}$$

Inductive Conformal Predictors framework always provides a valid prediction set under the assumption of exchangeability, which follows from i.i.d. assumption. Nevertheless, efficiency depends on chosen nonconformity measure and should be checked in each case. In our study, we use Gradient Boosting over Decision Trees as underlying algorithm. As nonconformity measure  $B(\zeta, (x, y)) = |y - \hat{f}(x)|$  was chosen [16, 17].

### 3.3. Clustering and visualization

In this section we give briefly methods description which were used in this study for exploratory data analysis. Cluster analysis and visualization of low-dimensional data representation help analyze spatial structure of the data and retrieve interesting insights.

#### 3.3.1. K-means clustering

Clustering is the technique of grouping a set of objects in metric space by distance. Usually one deals with normed vector space and objects represented as its numerical descriptions. One of the first clustering algorithms K-means had first proposed over 50 years ago. It is still one of the most widely used algorithms for clustering [18, 19]. Given  $n$  data points  $X = \{x_i\}_{i=1}^n \in \mathbf{X}^n \subset \mathbb{R}^{n \times d}$ , K-means is to group them into  $k$  clusters  $C = \{C_1, C_2, \dots, C_k\}$ . Let  $\mu_i = \frac{1}{|C_i|} \sum_{x \in C_i} x$  be the mean of the corresponding cluster  $C_i$  and each data point belongs to the cluster with the nearest mean. The goal of K-means is to minimize the sum of the squared distances between data points and its cluster means

$$\min_C \sum_{i=1}^k \sum_{x \in C_i} \|x - \mu_i\|^2.$$

At initial step random data points are selected as cluster means. Then the two following steps are repeated until convergence. The first step is to assign each data point to cluster with nearest mean. The second step is to recalculate cluster means corresponding to new partition. This algorithm finds a local minimum of the objective. Hence, result depends on initial guess. In our work we used an extension K-means++ which specifying a procedure to initialize cluster means [20]. Proposed initializing procedure makes algorithm stable and provides an optimal solution with strong chance.

#### 3.3.2. t-SNE

One of the common ways to visualize high-dimensional data is to find transformation from initial space into two or three-dimensional space with preserving spatial relationships. Well known PCA technique provides linear transformation to low dimensional space by finding the projections which maximize the variance. However, there are more effective non-linear methods to visualize the

spatial structure [21]. T-distributed Stochastic Neighbor Embedding (t-SNE) is a non-linear dimensionality reduction method which is widely used for high-dimensional datasets visualizing [22]. At first t-SNE computes  $p_{ij}$  that are proportional to similarity for every pair  $(x_i, x_j)$ :

$$p_{i|j} = \frac{\exp\left(\frac{-\|x_i - x_j\|^2}{2\sigma_i^2}\right)}{\sum_{k \neq i} \exp\left(\frac{-\|x_i - x_k\|^2}{2\sigma_i^2}\right)},$$

$$p_{ij} = \frac{p_{i|j} + p_{j|i}}{2d}.$$

Standard deviations  $\sigma_i$  are set using binary search in a way that the perplexity of the corresponding distribution is equal to the perplexity given by user. The perplexity can be interpreted as a smooth measure of the nearby points number. The similarity in low dimensional space is defined using Cauchy distribution:

$$q_{ij} = \frac{(1 + \|y_i - y_j\|^2)^{-1}}{\sum_{k \neq l} (1 + \|y_k - y_l\|^2)^{-1}}.$$

Low dimensional representations  $y_i$  are determined by minimizing Kullback-Leibler divergence between a joint probability distribution  $P$ , in the high-dimensional space and a joint probability distribution  $Q$ , in the low-dimensional space

$$KL(P\|Q) = \sum_i \sum_j p_{ij} \log\left(\frac{p_{ij}}{q_{ij}}\right).$$

In other words, algorithm finds a map which placed similar objects nearby in a low-dimensional space while keeping dissimilar objects well separated. Thus, this method is suitable to visualize clustering structure.

#### 4. Methodology

The proposed approach has several potential advantages over traditional recovery factor estimation methods. It is computationally efficient, allows to work with partial input and provides prediction uncertainty. However, it is necessary to evaluate its accuracy, validity and efficiency. Usually, reserves-estimation methods are divided into two classes: for pre-production phases and post-production phases. The main difference between these two classes is the type of data used. Methods related to pre-production phases usually predate development planning [2]. These methods generally entail more significant errors and uncertainty, and the economic effect can be greater compared to post-production techniques. Similarly, we build and evaluate two data-driven models. First one takes a set of parameters available at pre-production steps as input. The second one takes an extended set of parameters as input, including production data and development scheme description. We evaluate models with commonly used cross-validation technique. In the following sections, we describe both models design and evaluation details.

#### 4.1. Model for pre-production phases

At pre-production phases, one of the main objective is to estimate economic potential of the oilfield. Secondary oil recovery factor estimation is an essential step for asset valuation. On this stage usually only static parameters available such as geometric, transport and fluid properties. Using this data reserves need to be assessed as accurately as possible. However, recovery factor strongly depends on economic effect that is difficult to forecast. Hence, training set should contain oil reservoirs which were developing in diverse economic environments and with different technologies. In order to increase training set diversity, we build a training set using two sources of data: TORIS dataset and proprietary dataset. We identified similar parameters of these two sources and converted measurements to common units. We divide parameters in the combined dataset into two groups:

- Not suitable for pre-production model input — Production rate (current, oil tons per day), Well spacing (field averaged,  $km^2$ ), Pressure (current, atm), Well count (total production), Well count (total injection), Production (cumulative oil, mln tons)
- Suitable for pre-production model input — Thickness (net pay average, m), Net/gross ratio (average), Porosity (matrix average, %), Water saturation (average, %), FVF (oil,  $m^3$  in reservoir conditions/ $m^3$  in standard conditions), Depth (top reservoir, m TVD), Temperature (original, deg. C), Pressure (original, atm), Permeability (air average, mD), Reservoir age (mln years), API gravity (average, tons/ $m^3$ ), Viscosity (cp), Water salinity (ppm), Reserves (original oil in-place, mln tons), Gas/oil ratio (initial,  $m^3$  in standard conditions/tons), Lithology (main), Structural dip (degree)

Parameters from the first group usually are not available at pre-production phases, while parameters from the second group could be estimated with several appraisal wells.

Both sources present estimated secondary oil recovery factors. The more depleted reservoir, the more reliable recovery factor estimation we have in the dataset. The purpose is to develop technique for estimating actual economic potential of the oil reservoir. Therefore, we consider only reservoirs which are close to depletion ( $\geq 90\%$  of oil reserves had extracted). To perform cluster analysis and to analyze the spatial structure of the data, we consider records with not more than one missing value.

Cluster analysis helps to find groups of objects (clusters) that are similar to each other. As a similarity measure, we use euclidean distance for scaled parameters. We perform cluster analysis and identify the number of clusters. We visualize spatial structure with t-SNE algorithm and provide analysis of parameters distributions for each cluster. For each cluster as well as for the full training set, we calculate evaluation metrics with cross-validation. Thus, we compare and evaluate two considered algorithm and analyze the prediction quality for each cluster.

#### 4.2. Model for post-production phases

During post-production phases, additional information about an oil reservoir becomes available, such as development details, production dynamic and other updated measurements. We consider the proprietary database as the only source for training set building. It includes a more detailed oil reservoirs descriptions with timestamps of the measurements made during the production phases. We do not consider items with more than 50% missing values. The following parameters have selected as input:

Onshore or offshore, Elevation (m), Water depth (m), Hydrocarbon type (main), Discovery year, Reservoir status, Well count (total production), Well count (total injection), Seismic anomaly, True vertical depth (top of reservoir, m), Structural dip (degree), Area (original productive,  $km^2$ ), Fluid contact (original, m TVD), Hydrocarbon column height (original oil, m), Hydrocarbon column height (original total, m), Reservoir age, Depositional system (main), Depositional environment (main), Stratigraphic compartment count, Lithology (main), Thickness (gross average, m), Net/gross ratio (average), Thickness (net pay average, m), Porosity (matrix avg, min, max %), Permeability (air avg, min, max mD), Water saturation (avg, min, max %), TOC (avg, min, max %), Kerogen type, Reserves (original in-place oil, mln tons), Reserves (original in-place oil equivalent, mln tons), Production year (cumulative), Production (cumulative oil, mln tons), Production year (start), Well count (current producing), Well count (current injection), Water-cut (current %), Production rate (current oil, tons per day), API gravity (average deg. API), Viscosity (cp), Viscosity temperature (deg. C), Sulphur (%), Gas/oil ratio (initial m<sup>3</sup> in standard conditions / tons), FVF (oil m<sup>3</sup> in reservoir conditions / m<sup>3</sup> in standard conditions), Temperature (original deg. C), Temperature depth (m), Pressure (original atm), Pressure depth (m), Pressure (current atm), Pressure gradient (original atm/m), Pressure (saturation atm), Water salinity (ppm), Improved recovery method (secondary), Well spacing (oil average  $km^2$ )

We use target encoding technique to transform categorical parameters in a numeric form. It replaces each category by average oil recovery factor among this category. Since we are considering oil reservoirs during production phases, a ratio of cumulative oil production ( $P$ ) to original oil in place ( $V$ ) gives a lower bound to estimated oil recovery factor ( $rf$ ) as shown in Figure 3. General analysis of the production behaviour of all oil reservoirs in training set can help to estimate margin between  $\frac{P}{V}$  and  $rf$ . Denote  $\Delta t$  as difference between “Production year (cumulative)” and “Production year (start)”. Then, approximation of the function  $\hat{f}(\Delta t, V, \mathbf{w}^*) \approx \frac{P(\Delta t)}{rf*V}$  could give an approximation of the oil recovery factor as  $\hat{rf}(P(\Delta t), \Delta t, V) \approx \frac{P(\Delta t)}{\hat{f}(\Delta t, V, \mathbf{w}^*)*V}$ , where  $\mathbf{w}$  are tunable parameters, which can be selected with mean squared error minimization

$$\mathbf{w}^* = \arg \min_{\mathbf{w}} \frac{1}{n} \sum_{i=1}^n \left( \frac{P_i(\Delta t_i)}{V_i * \hat{f}(\Delta t_i, V_i, \mathbf{w})} - rf_i \right)^2.$$

$\hat{f}(\Delta t, V, \mathbf{w}^*)$  should meet the same conditions as  $\frac{P(\Delta t)}{rf*V}$ , i.e.

$$\hat{f}(\Delta t, V, \mathbf{w}^*) \rightarrow 1, \quad \Delta t \rightarrow +\infty, \quad (2)$$

$$\hat{f}(0, V, \mathbf{w}^*) = 0. \quad (3)$$

This approach allows us to generate informative extra features for any machine learning algorithm using different functional families. Similarly to known cumulative oil production curves equations [23], we consider  $\hat{f}(\Delta t, V, \mathbf{w}^*)$  as exponential and hyperbolic functional families. Tunable parameters  $\mathbf{w}^*$  can be found by minimizing error on a training set, then extra feature can be calculated both for training and test set as  $\hat{r}f(P(\Delta t), \Delta t, V)$ .

Overall, the first step is to make data preprocessing in the way described above. The second step is to conduct an analysis of the production dynamic and select appropriate functional families for generating extra features to improve predictive models accuracy. The third step is evaluation and comparison of the Quantile Regression Forest and Gradient Boosting over decision trees with Inductive Conformal Predictors using different extra features subsets.

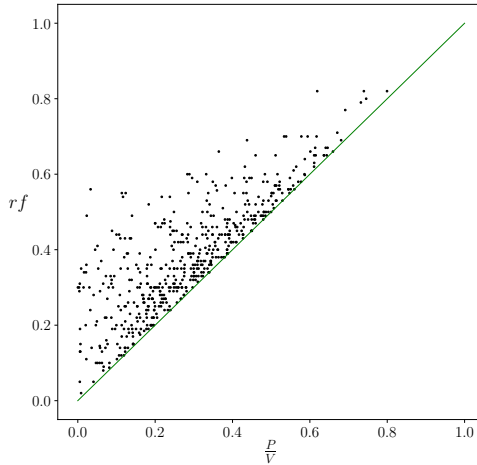


Figure 3: Scatter plot shows that ratio of cumulative oil production ( $P$ ) and original oil in place ( $V$ ) gives a close lower bound to oil recovery factor ( $rf$ ).

#### 4.3. Evaluation metrics

To evaluate accuracy, validity and efficiency of the considering models we use cross-validation. Cross-validation is primarily used in machine learning to estimate generalization ability of the algorithm. The procedure is as follows: randomly shuffle the data, split the data into  $K$  groups, each group is considered as a test set and the remaining part — as a train set. Since each data point

would be considered as a test point, we obtain predictions of a model for all datapoints. Denote  $\hat{y}$ ,  $\hat{l}^\alpha$  and  $\hat{u}^\alpha$  as vectors of predictions, lower bounds and upper bounds of the prediction intervals on confidence level  $\alpha$  obtained on cross-validation respectively. To show the error of predictions we use the following metrics:

$$\text{Mean average error (MAE)} : \text{MAE}(\hat{y}, y) = \frac{1}{n} \sum_{i=1}^n |y_i - \hat{y}_i|,$$

$$\text{Coefficient of determination (R}^2\text{)} : R^2(\hat{y}, y) = 1 - \frac{\sum_{i=1}^n (\hat{y}_i - y_i)^2}{\sum_{j=1}^n (\frac{1}{n} \sum_{k=1}^n y_k - y_j)^2}.$$

To evaluate the validity of the prediction intervals we calculate the coverage rate, which should be greater or equal than confidence level  $\alpha$ :

$$\frac{1}{n} \sum_{i=1}^n \mathbb{I}_{\hat{l}_i^\alpha \leq y_i \leq \hat{u}_i^\alpha}.$$

To evaluate the efficiency of the prediction intervals, we calculate its mean width. The less mean width, the more informative prediction intervals.

$$\frac{1}{n} \sum_{i=1}^n |\hat{u}_i^\alpha - \hat{l}_i^\alpha|$$

## 5. Results & Discussion

### 5.1. Model for pre-production phases

To build the prediction model for pre-production phases, we combine and filter both datasets: TORIS and proprietary. The resulting training set contains 407 oil reservoirs, described by 16 time-independent parameters. We perform an analysis of the spatial structure of the training set using clustering technique K-means and t-SNE algorithm for data visualization. Cluster analysis indicated the presence of two clusters in original space. Two-dimensional embeddings from the training set obtained with t-SNE depicted in Figure 4. This embeddings visualization confirms the presence of two clusters. K-means partition is consistent with the observed cluster structure in embedded space, Figure 4a. Figure 4b shows that cluster #1 contains oil reservoirs from Proprietary dataset as well as from TORIS dataset. Cluster #2 contains oil reservoirs primarily from TOIRS dataset. Therefore, reservoirs from cluster #2 geographically located primarily in North America. On the other hand, reservoirs from the cluster #1 have more geographic diversity. Comparison of parameters distributions for each cluster shows that cluster #1 contains reservoirs with higher porosity and permeability, than cluster #2. A significant difference is observed in the geological age of the rock (see Figure 5). Also, clusters differ in main sediments. Most of the reservoirs from cluster #1 (98 %) are terrigenous. By contrast,

most of the reservoirs from cluster #2 (65 %) are carbonate. On both clusters, as well as on entire training set, we evaluate the considered machine learning algorithms. Table 1 and Figure 6 demonstrate that recovery factor predictions are more accurate for cluster #1. Gradient Boosting with ICP and Quantile Regression Forests both provides prediction intervals close to valid, Table 2. Gradient Boosting with ICP demonstrates the most accurate result, Table 1.

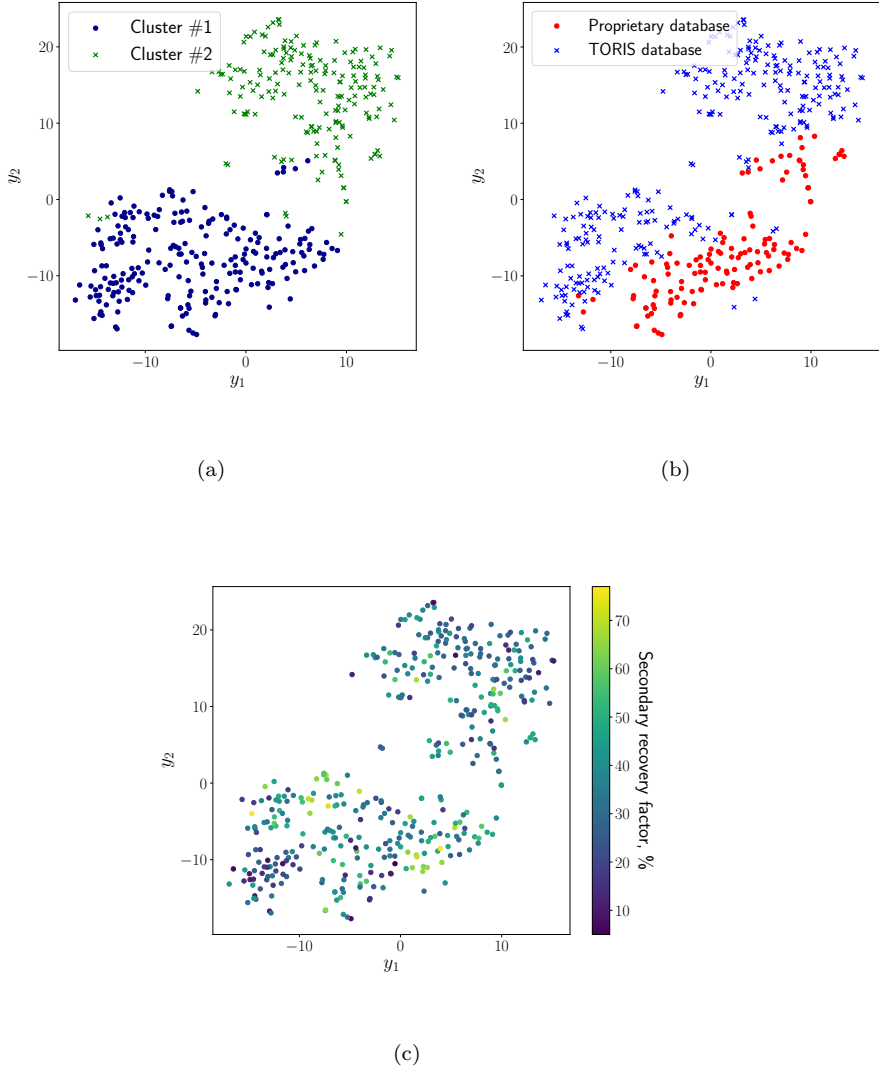


Figure 4: Two dimensional t-SNE training set embeddings visualisations. T-sne transforms training set into two-dimensional space with preserving spatial relationships. Figure 4a demonstrates result of K-means partitioning in original space. K-means partition is consistent with the observed cluster structure in embedded space. Figure 4b demonstrates data sources of the oil reservoirs descriptions. Figure 4c demonstrates distribution of secondary oil recovery factor.

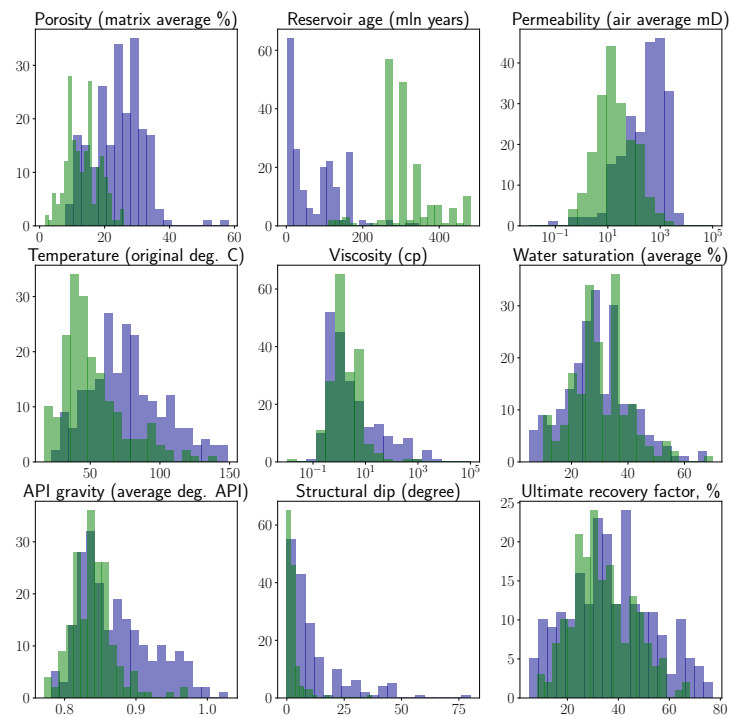


Figure 5: Plots demonstrate most distinguishable parameters distributions for each cluster.  
 Blue color - histograms for cluster #1. Green color - histograms for cluster #2.

Gradient Boosting			
Cluster #	1	2	1&2
MAE	9.57	8.63	9.06
$R^2$	0.47	0.1	0.38
Random Forests			
Cluster #	1	2	1&2
MAE	9.93	8.80	9.13
$R^2$	0.45	0.09	0.38

Table 1: Comparison of Gradient Boosting and Random Forests algorithm on both clusters, as well as on entire training set. Error metrics calculated on leave one out cross-validation. Listed metrics demonstrate more accurate results for cluster #1 in terms of  $R^2$ . Mean absolute error for cluster #2 is less than for the cluster #1, but that is due to lower oil recovery factor range in the cluster #2.

Gradient Boosting with ICP									
Cluster #	1			2			1&2		
$\alpha$	0.7	0.8	0.9	0.7	0.8	0.9	0.7	0.8	0.9
Mean width	24.91	31.36	42.05	25.80	33.49	47.03	24.69	30.41	40.41
Coverage	0.66	0.77	0.87	0.72	0.86	0.95	0.70	0.81	0.91
Quantile Regression Forests									
Cluster #	1			2			1&2		
$\alpha$	0.7	0.8	0.9	0.7	0.8	0.9	0.7	0.8	0.9
Mean width	25.75	31.66	39.85	20.28	25.13	32.74	23.50	29.17	37.10
Coverage	0.70	0.82	0.87	0.66	0.77	0.86	0.71	0.81	0.89

Table 2: Mean width and coverage rate calculated on leave one out cross-validation.

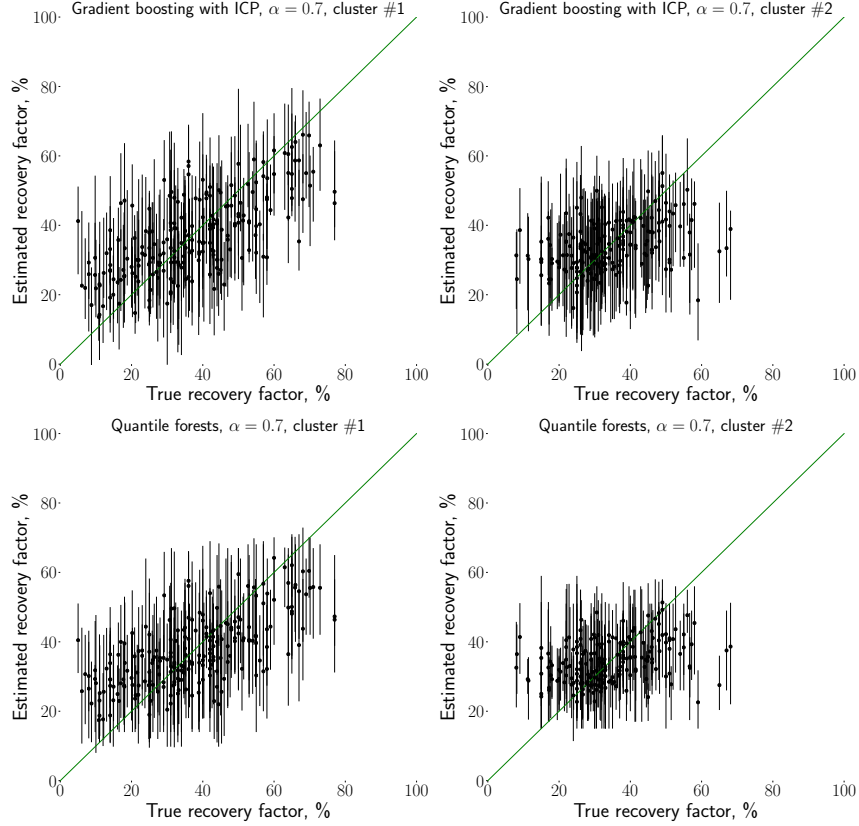


Figure 6: Prediction intervals visualization for 70% confidence level. The graphs show randomly picked 25% points from leave one out cross-validation.

### 5.2. Model for post-production phases

To build the prediction model for post-production phases, we use proprietary database only since it contains a comprehensive description of oil reservoirs as well as timestamps of the current measurements. The resulting training set contains 549 oil reservoirs, each of which is described by 67 parameters. Due to a large number of parameters (curse of dimensionality) and a high portion of the missing values, we do not perform cluster analysis. First of all, we analyzed the accuracy of recovery factor estimation with general production curves  $\hat{f}(\Delta t, V, w^*)$  as an approximation of  $\frac{P(\Delta t)}{r_f^* V}$ . We search approximation in exponential and hyperbolic functional families. The first group of functional families depends only on  $\Delta t$ :

$$f_{hyp}(\Delta t, w) = \frac{\Delta t}{\Delta t + w},$$

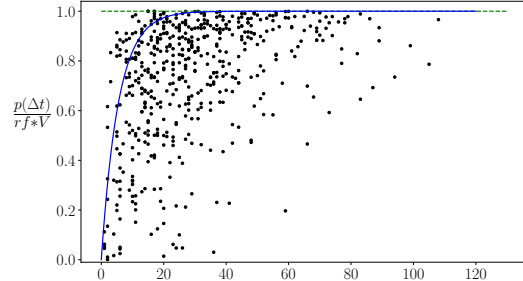
$$f_{exp}(\Delta t, w) = 1 - e^{-\frac{\Delta t}{w}}.$$

For both families, parameter  $w$  determines the slope of the curve. Figure 7a demonstrates optimal curve from exponential functional family. Since reservoirs with large original oil in place are deplete more slowly, their production curve slope will be more shallow. Figure 7b shows that parameter  $w$  directly depends on original oil in place ( $V$ ). Figure 7c demonstrate type of this dependency. Thus, we consider the second group of functional families. Adding dependence on original oil in place ( $V$ ), we obtain more complex models:

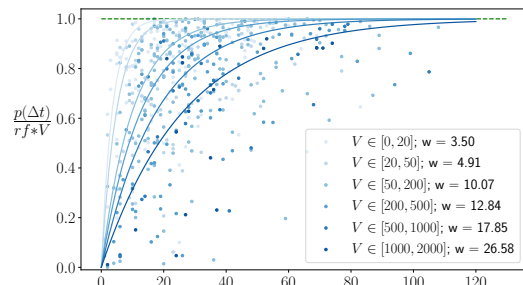
$$f_{hyp}(\Delta t, V, w_0, w_1) = \frac{\Delta t}{\Delta t + w_1 \sqrt{V} + w_0},$$

$$f_{exp}(\Delta t, V, w_0, w_1) = 1 - e^{-\frac{\Delta t}{w_1 \sqrt{V} + w_0}}.$$

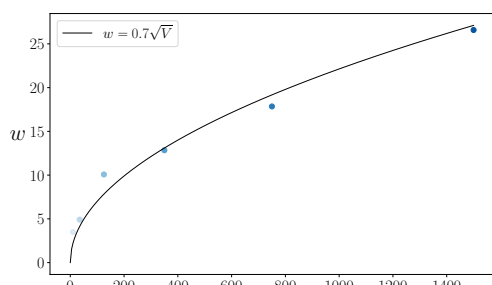
Using a training set and any optimization algorithm, we can find an approximation of the general production curve in a functional space. This approximation could be used for oil recovery factor estimation with knowing  $dt$ ,  $V$  and  $P$ . Table 3 lists the oil recovery factor errors metrics on cross-validation for different functional families. As a baseline, the table also shows errors metrics for the simplest oil recovery factor estimation:  $\frac{P}{V}$ . It is easy to see that the general production curve approach approximation from hyperbolic functional family is much accurate than baseline  $\frac{P}{V}$ . To enhance the predictive accuracy of machine learning models, we use the oil recovery factor approximations from general production curves as an extra input (this approach is also known as stacking). As potential extra input features we consider  $\frac{P}{V}$ ,  $rf_{exp}(\Delta t, P)$ ,  $rf_{exp}(\Delta t, V, P)$ ,  $rf_{hyp}(\Delta t, P)$ ,  $rf_{hyp}(\Delta t, V, P)$ .



(a)



(b)



(c)

Figure 7: Figure 7a shows general production curve approximation found with mean squared error minimization in exponential functional family  $f_{exp}(\Delta t, w) = 1 - e^{-\frac{\Delta t}{w}}$ . Figure 7b demonstrates curves found for oil reservoirs groups with various amount of original oil in place. Figure 7c shows that dependence between original oil in place and  $w$  can be approximated with square root. Identical situation in case of hyperbolic functional family.

	$\frac{P}{V}$	$rf_{exp}(\Delta t, P)$	$rf_{exp}(\Delta t, V, P)$	$rf_{hyp}(\Delta t, P)$	$rf_{hyp}(\Delta t, V, P)$
MAE	10.13	9.33	8.64	8.26	7.78
$R^2$	0.12	0.23	0.29	0.35	0.44

Table 3: Oil recovery factor error metrics using general production curve approximation from different functional families in comparison with simplest baseline  $\frac{P}{V}$ .

Table 4 demonstrates the synergy effect from the combination of general production curves estimation approach and machine learning models. There is a significant improvement in accuracy with using the following extra features subset  $\frac{P}{V}$ ,  $rf_{exp}(\Delta t, V, P)$  and  $rf_{hyp}(\Delta t, V, P)$ . Table 5 demonstrates prediction intervals validity and lists its mean width for both Gradient Boosting with ICP and Quantile Regression Forests. Figure 8 depicts prediction intervals at 80% and 95% confidence levels for both algorithms.

Gradient Boosting					
Extra features	-	$\frac{P}{V}$	$rf_{exp}(\Delta t, V, P)$	$rf_{hyp}(\Delta t, V, P)$	$\frac{P}{V}, rf_{exp,hyp}(\Delta t, V, P)$
MAE	8.56	5.13	5.29	5.08	<b>4.91</b>
$R^2$	0.48	0.78	0.77	0.79	<b>0.80</b>
Random Forests					
Extra features	-	$\frac{P}{V}$	$rf_{exp}(\Delta t, V, P)$	$rf_{hyp}(\Delta t, V, P)$	$\frac{P}{V}, rf_{exp,hyp}(\Delta t, V, P)$
MAE	9.45	5.55	5.63	5.47	5.30
$R^2$	0.37	0.75	0.75	0.77	0.78

Table 4: Table lists error metrics calculated on 20 fold cross-validation. It shows effect from adding  $\frac{P}{V}$  (ratio of cumulative oil production to original oil in place),  $rf_{exp}(\Delta t, V, P)$  (recovery factor estimation based on general production curve from exponential functional family) and  $rf_{hyp}(\Delta t, V, P)$  (recovery factor estimation based on general production curve from hyperbolic functional family). The last column relates to adding subset of all three features.

$\alpha$	GB with ICP			QRF		
	0.8	0.9	0.95	0.8	0.9	0.95
Mean width	18.01	24.76	32.66	17.39	22.48	26.61
Coverage	0.80	0.9	0.95	0.84	0.91	0.94

Table 5: Mean width and coverage rate calculated on 20 fold cross-validation. Both models appears to be valid, since coverage rates are close to corresponding confidence levels.

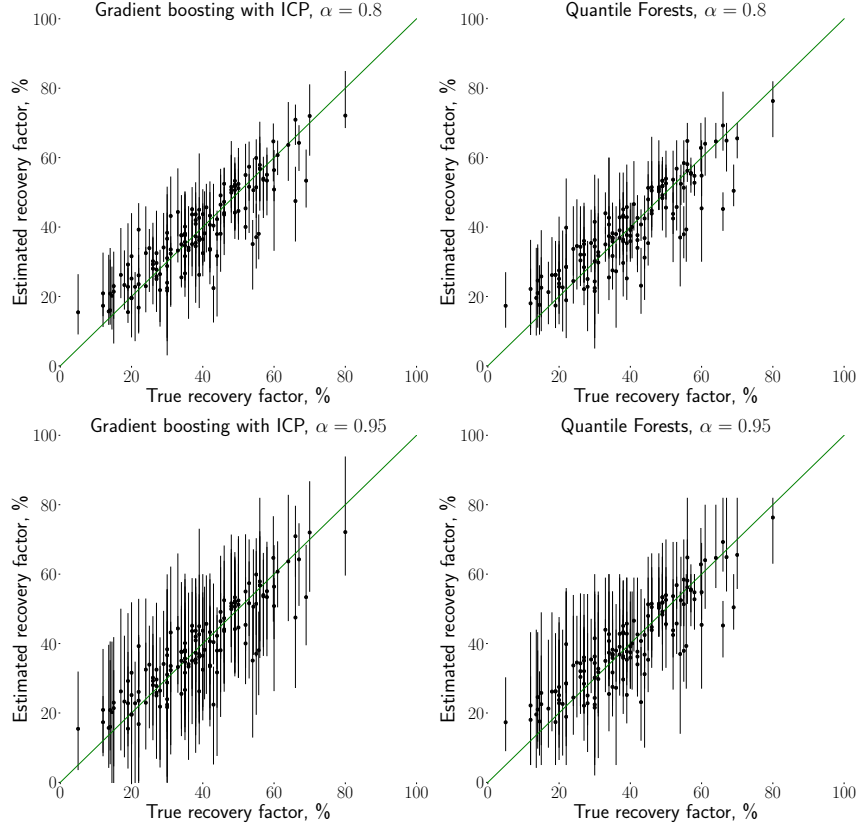


Figure 8: Prediction intervals visualization for 80% and 95% confidence levels. Depicted results for randomly picked 25% points from 20 fold cross-validation.

### 5.3. Discussion

In this work, we built and evaluated two tree-based uncertainty quantification models in application to estimating secondary recovery factor. We conducted a separate analysis for pre-production phases case and post-production phases. For the pre-production phases case, we conducted a cluster analysis and identified two groups of oil reservoirs. Reservoirs from the first group (cluster) are characterized by less than 200 million years geological age, predominantly terrigenous deposits, relatively high porosity and permeability. Prediction models demonstrate relatively accurate results for this group and can be used by reservoir experts to assess the potential of the hydrocarbon reservoirs. The best results showed Gradient Boosting with  $MAE = 9.57$  and  $R^2 = 0.47$ . For the second group, models proved to be less accurate than for the first group. The best metrics shows Gradient Boosting:  $MAE = 8.63$  and  $R^2 = 0.1$ . For both

cases, models provide reliable predictive intervals.

For the post-production phases, we consider additional information about an oil reservoir as predictors: development details, production dynamic and other updated measurements. We showed that the proposed general production curve approximation technique helps significantly increase the accuracy of predictive models. We use exponential and hyperbolic functional families to approximate general production curves and use the stacking technique to combine these models with tree-based ensembles. The best model demonstrates the following error metrics calculated on cross-validation:  $MAE = 4.91$  and  $R^2 = 0.8$ . It also provides reliable predictive intervals. Overall, the model demonstrates predictive power and capability to help experts to optimize development plan as well as to validate results of the hydrodynamic model.

The data-driven technique might be used as a tool for the prompt and objective assessment of reservoir potential due to the richness of the data used for training. It requires much less time and efforts to estimate recovery factor in comparison to existing mature and standard methods. In addition, there is an option to use partial input data for the oil reservoir for assessment. Another advantage of the prediction model is the ability to estimate prediction intervals for the corresponding confidence levels. The trained model generates the recovery factor prediction and calculates the error within a fraction of a second on just a modern office laptop which is orders of magnitude faster than the most advanced 2D [24] and 3D [25, 26, 27] reservoir models combining differential equations and deep learning techniques. Overall, machine learning has demonstrated its capability to assess the potential of the hydrocarbon reservoirs. Additional data about different types of reservoirs could allow building more accurate predictive models. Several authors have considered dataset development using design of experiment methods and hydrocarbon reservoir simulators. A notable examples of this approach are presented in [28] and [29]. The future research will consider ways to increase training set size using hydrodynamic simulators or its surrogate models [27].

## References

- [1] Z. Rui, J. Lu, Z. Zhang, R. Guo, K. Ling, R. Zhang, S. Patil, A quantitative oil and gas reservoir evaluation system for development, *Journal of Natural Gas Science and Engineering* 42 (2017) 31–39. doi:<https://doi.org/10.1016/j.jngse.2017.02.026>.
- [2] F. Demirmen, et al., Reserves estimation: the challenge for the industry, *Journal of Petroleum Technology* 59 (2007) 80–89.
- [3] H. Li, H. Yu, N. Cao, H. Tian, S. Cheng, Applications of artificial intelligence in oil and gas development, *Archives of Computational Methods in Engineering* (2020) 1–13.
- [4] R. Guthrie, M. H. Greenberger, et al., The use of multiple-correlation analyses for interpreting petroleum-engineering data, in: *Drilling and Production Practice*, American Petroleum Institute, 1955.
- [5] J. Arps, F. Brons, A. Van Everdingen, R. Buchwald, A. Smith, A statistical study of recovery efficiency, *Bull. D* 14 (1967).
- [6] A. Sharma, S. Srinivasan, L. W. Lake, et al., Classification of oil and gas reservoirs based on recovery factor: a data-mining approach, in: *SPE Annual Technical Conference and Exhibition*, Society of Petroleum Engineers, 2010. doi:<http://dx.doi.org/10.2118/130257-MS>.
- [7] A. A. Mahmoud, S. Elkhatatny, W. Chen, A. Abdulraheem, Estimation of oil recovery factor for water drive sandy reservoirs through applications of artificial intelligence, *Energies* 12 (2019) 3671.
- [8] B. Han, X. Bian, A hybrid pso-svm-based model for determination of oil recovery factor in the low-permeability reservoir, *Petroleum* 4 (2018) 43–49.
- [9] K. Aliyuda, J. Howell, Machine-learning algorithm for estimating oil-recovery factor using a combination of engineering and stratigraphic dependent parameters, *Interpretation* 7 (2019) SE151–SE159. doi:<https://doi.org/10.1190/INT-2018-0211.1>.
- [10] M. Belyaev, E. Burnaev, E. Kapushev, M. Panov, P. Prikhodko, D. Vetrov, D. Yarotsky, Gtapprox: Surrogate modeling for industrial design, *Advances in Engineering Software* 102 (2016) 29 – 39. doi:<https://doi.org/10.1016/j.advengsoft.2016.09.001>.
- [11] L. Breiman, Random forests, *Machine learning* 45 (2001) 5–32. doi:<https://doi.org/10.1023/A:1010933404324>.
- [12] J. J. Rodriguez, L. I. Kuncheva, C. J. Alonso, Rotation forest: A new classifier ensemble method, *IEEE transactions on pattern analysis and machine intelligence* 28 (2006) 1619–1630. doi:<http://dx.doi.org/10.1109/TPAMI.2006.211>.

- [13] N. Meinshausen, Quantile regression forests, *Journal of Machine Learning Research* 7 (2006) 983–999.
- [14] J. H. Friedman, Greedy function approximation: a gradient boosting machine, *Annals of statistics* (2001) 1189–1232. doi:<https://doi.org/10.1214/aos/1013203451>.
- [15] V. Vovk, A. Gammerman, G. Shafer, *Algorithmic learning in a random world*, Springer Science & Business Media, 2005. doi:<https://doi.org/10.1007/b106715>.
- [16] E. Burnaev, V. Vovk, Efficiency of conformalized ridge regression, in: M. F. Balcan, V. Feldman, C. Szepesvári (Eds.), *Proceedings of The 27th Conference on Learning Theory*, volume 35 of *Proceedings of Machine Learning Research*, 2014, pp. 605–622.
- [17] E. Burnaev, I. Nazarov, Conformalized kernel ridge regression, in: 2016 15th IEEE International Conference on Machine Learning and Applications (ICMLA), 2016, pp. 45–52. doi:<10.1109/ICMLA.2016.0017>.
- [18] J. A. Hartigan, M. A. Wong, Algorithm as 136: A k-means clustering algorithm, *Journal of the Royal Statistical Society. Series C (Applied Statistics)* 28 (1979) 100–108. doi:<http://dx.doi.org/10.2307/2346830>.
- [19] A. K. Jain, Data clustering: 50 years beyond k-means, *Pattern recognition letters* 31 (2010) 651–666. doi:<http://dx.doi.org/10.1016/j.patrec.2009.09.011>.
- [20] D. Arthur, S. Vassilvitskii, k-means++: The advantages of careful seeding, in: *Proceedings of the eighteenth annual ACM-SIAM symposium on Discrete algorithms*, Society for Industrial and Applied Mathematics, 2007, pp. 1027–1035.
- [21] W. Li, J. E. Cerise, Y. Yang, H. Han, Application of t-sne to human genetic data, *Journal of bioinformatics and computational biology* 15 (2017) 1750017. doi:<https://doi.org/10.1142/S0219720017500172>.
- [22] L. v. d. Maaten, G. Hinton, Visualizing data using t-sne, *Journal of machine learning research* 9 (2008) 2579–2605.
- [23] M. Fetkovich, E. Fetkovich, M. Fetkovich, et al., Useful concepts for decline curve forecasting, reserve estimation, and analysis, *SPE Reservoir Engineering* 11 (1996) 13–22. doi:<http://dx.doi.org/10.2118/28628-PA>.
- [24] Z. L. Jin, Y. Liu, L. J. Durlofsky, Deep-learning-based reduced-order modeling for subsurface flow simulation, *arXiv preprint arXiv:1906.03729* (2019).

- [25] P. Temirchev, M. Simonov, R. Kostoev, E. Burnaev, I. Oseledets, A. Akhmetov, A. Margarit, A. Sitnikov, D. Koroteev, Deep neural networks predicting oil movement in a development unit, *Journal of Petroleum Science and Engineering* 184 (2020) 106513.
- [26] M. Simonov, A. Akhmetov, P. Temirchev, D. Koroteev, R. Kostoev, E. Burnaev, I. Oseledets, et al., Application of machine learning technologies for rapid 3d modelling of inflow to the well in the development system, in: *SPE Russian Petroleum Technology Conference*, Society of Petroleum Engineers, 2018.
- [27] P. Temirchev, A. Gubanova, R. Kostoev, A. Gryzlov, D. Voloskov, D. Koroteev, M. Simonov, A. Akhmetov, A. Margarit, A. Ershov, et al., Reduced order reservoir simulation with neural-network based hybrid model, in: *SPE Russian Petroleum Technology Conference*, Society of Petroleum Engineers, 2019.
- [28] M. Naderi, E. Khamehchi, Nonlinear risk optimization approach to water drive gas reservoir production optimization using doe and artificial intelligence, *Journal of Natural Gas Science and Engineering* 31 (2016) 575–584.
- [29] P. Panja, R. Velasco, M. Pathak, M. Deo, Application of artificial intelligence to forecast hydrocarbon production from shales, *Petroleum* 4 (2018) 75–89.